Papers in Honour of Ken Aplin

edited by

Julien Louys, Sue O'Connor and Kristofer M. Helgen

Records of the Australian Museum

volume 72, issue no. 5

25 November 2020

AUSTRALIAN MUSEUM

Records of the Australian Museum (2020)
vol. 72, issue no. 5, pp. 161–174
https://doi.org/10.3853/j.2201-4349.72.2020.1732

Records of the Australian Museum
a peer-reviewed open-access journal
published by the Australian Museum, Sydney
communicating knowledge derived from our collections
ISSN 0067-1975 (print), 2201-4349 (online)

A New Species of Extinct False Vampire Bat (Megadermatidae: *Macroderma*) from the Kimberley Region of Western Australia

Kyle N. Armstrong[1,2,3], Ken Aplin[1,4]†, and Masaharu Motokawa[1]

[1] The Kyoto University Museum, Yoshida Honmachi, Sakyo-ku, Kyoto, 606-8501, Japan

[2] School of Biological Sciences, The University of Adelaide SA 5005, Australia

[3] South Australian Museum, North Terrace, Adelaide SA 5000, Australia

[4] Australian Museum Research Associate, 1 William Street, Sydney NSW 2010, Australia

Abstract. A new species of False Vampire Bat (Megadermatidae), *Macroderma handae* sp. nov., is described from dental, dentary and maxillary fragments recovered from limestone deposits at Dingo Gap, Oscar Range, in the Kimberley region of Western Australia. This material is likely to be of Pliocene age, or early Pleistocene, based on biocorrelation within the same sample. The absence of the P^2 indicates that it is more derived than Miocene taxa including *M. malugara* and *M. godthelpi*, but its phylogenetic position relative to *M. koppa* could not be determined. It appears to be slightly smaller than *M. gigas* and *M. koppa* based on the size of M^1 and M_2. It can be distinguished from *M. gigas* by the lesser degree of fenestration in the maxilla; and from all other species of *Macroderma* by the shape of the protofossa of the M^1, plus the M_2 protoconid relatively high and of proportionally greater area within the trigonid. Other material collected, but not identified completely or described, includes several lower canines from a species of emballonurid, and a dentary with M_{1-3} representing a vespertilionid bat. Given the wear striations observed on the M_3 of the newly-described *Macroderma* species, we suggest that it was a predator of small vertebrates, including possibly the chiropteran co-inhabitants of the cave. This new species of *Macroderma* is the sixth species recognized in the genus so far, and the second from the Pliocene.

Introduction

The family Megadermatidae (False Vampire Bats) has a long history that began in the mid-Eocene with its divergence from the Craseonycteridae c. 44–43 Ma, based on molecular dating methods (95% credibility interval 47–39 Ma; Teeling *et al.*, 2005; Foley *et al.*, 2015). Until recently, the oldest known megadermatid fossil was considered to be *Necromantis adichaster* Weithofer, 1887, represented in the Quercy Phosphorites Formation, France, but this genus is now accepted to be part of a distinct family (Necromantidae; Sigé, 2011; Ravel *et al.*, 2016; Hand & Sigé, 2018). Early megadermatid lineages are represented by modern extant taxa in the genera *Lavia* and *Cardioderma*, based on their inferred phylogenetic position (Hand, 1985; but see Kaňuch *et al.*, 2015). The oldest megadermatid fossils, however, are: *Saharaderma pseudovampyrus* Gunnell *et al.*, 2008 from early Oligocene deposits in Egypt (33.9–28.4 Ma), which shows similarities to *Cardioderma* and *Lavia*, and with which it may form a distinct African clade (Gunnell *et al.*, 2008); and *Megaderma lopezae* Sevilla, 1990 from early Oligocene deposits in Spain. The remaining eight described Afro-European species of extinct *Megaderma* are represented in deposits that range

Keywords: *Macroderma*; *Megaderma*; Ghost Bat; False Vampire Bat; new species; Pliocene
Taxonomic registration: urn:lsid:zoobank.org:pub:D252FDFE-7C93-4E13-8DC7-FFB585ACC16F
Corresponding author: Kyle N. Armstrong kyle.armstrong@adelaide.edu.au
Received: 3 February 2020 **Accepted**: 20 August 2020 **Published**: 25 November 2020 (in print and online simultaneously)
Publisher: The Australian Museum, Sydney, Australia (a statutory authority of, and principally funded by, the NSW State Government)
Citation: Armstrong, Kyle N., Ken Aplin, and Masaharu Motokawa. 2020. A new species of extinct False Vampire Bat (Megadermatidae: *Macroderma*) from the Kimberley Region of Western Australia. In *Papers in Honour of Ken Aplin*, ed. Julien Louys, Sue O'Connor, and Kristofer M. Helgen. *Records of the Australian Museum* 72(5): 161–174. https://doi.org/10.3853/j.2201-4349.72.2020.1732

† Ken Aplin 1958–2019, deceased

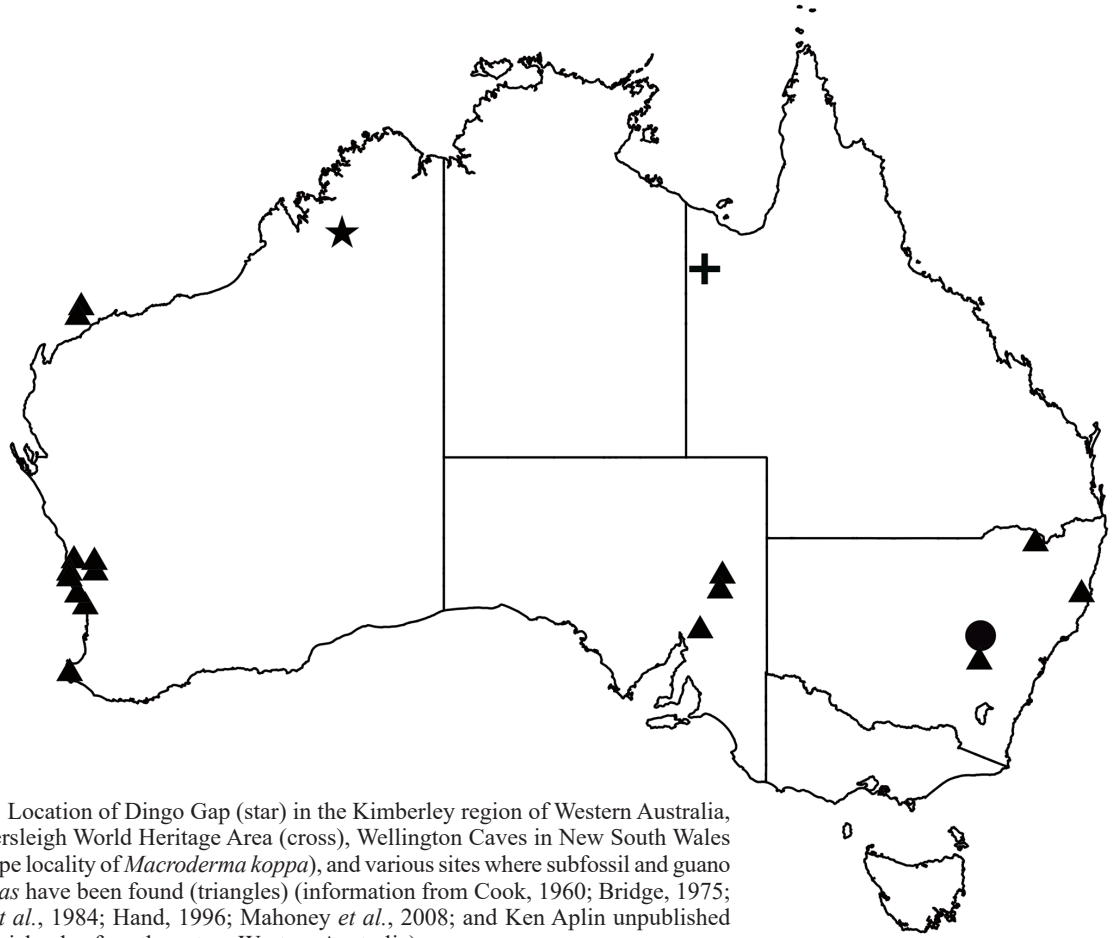

Figure 1. Location of Dingo Gap (star) in the Kimberley region of Western Australia, plus Riversleigh World Heritage Area (cross), Wellington Caves in New South Wales (circle; type locality of *Macroderma koppa*), and various sites where subfossil and guano of *M. gigas* have been found (triangles) (information from Cook, 1960; Bridge, 1975; Molnar *et al.*, 1984; Hand, 1996; Mahoney *et al.*, 2008; and Ken Aplin unpublished data from islands of northwestern Western Australia).

in age from the early Miocene (e.g., *Megaderma brailloni* Sigé, 1968 from the Aquitanian) to the Pleistocene (e.g., *Megaderma watwat* Bate, 1937) (reviewed in Sigé, 1976; Sevilla, 1990; Ziegler, 1993).

Australia has excellent representation of megadermatid fossil taxa, beginning from the mid-Cenozoic and extending to subfossil recent material (Molnar *et al.*, 1984; Hand, 1996). Most have been discovered in the freshwater limestone deposits of Riversleigh World Heritage Area, northwestern Queensland, which has a rich diversity of bat species from the families Mystacinidae (Hand *et al.*, 1998), Emballonuridae (Archer *et al.*, 2006; King, 2013), Rhinonycteridae (Sigé *et al.*, 1982; Hand, 1997a; Hand & Archer, 2005), Hipposideridae (Hand, 1997b; Hand, 1998a, 1998b), Molossidae (Hand, 1990; Hand *et al.*, 1997), and Vespertilionidae (Menu *et al.*, 2002).

The genus *Megaderma* is thought to have entered Australia after the middle Miocene, and the small-sized *Megaderma richardsi* from the early Pleistocene Rackham's Roost Site at Riversleigh is its only known representative in Australia (Hand, 1995; Woodhead *et al.*, 2016). Four extinct Australian megadermatid taxa have been referred to the endemic genus *Macroderma—M. godthelpi* Hand, 1985 from the early Miocene Microsite and middle Miocene Gag Site, Riversleigh; *M. malugara* Hand, 1996 from the middle Miocene Gotham City Site, Riversleigh; an unnamed species of *Macroderma* from the middle Miocene Henk's Hollow Site, Riversleigh (Hand, 1996); and *M. koppa* Hand, Dawson & Augee, 1988 from the Pliocene deposits of Big Sink, Wellington Caves, New South Wales (Hand *et al.*, 1988). The remaining two extinct megadermatid taxa from Australia have not been given a formal binomial name—Dwornamor Variant from the middle Miocene Gag Site, Riversleigh (Hand, 1985); and Megadermatidae indet. from the middle Miocene Henk's Hollow Site, Riversleigh (Hand, 1996).

The extant *Macroderma gigas* (Dobson, 1880) is currently distributed across northern Australia, from the Pilbara and Kimberley regions of Western Australia, through the Top End of the Northern Territory and part of the Gulf Coastal and Mt Isa Inlier bioregions of the Northern Territory and northwestern Queensland, to Cape York, Queensland (Worthington Wilmer *et al.*, 1999; Churchill, 2008). It contracted from areas further south in the Holocene (Molnar *et al.*, 1984), and has declined further since the arrival of Europeans (Churchill & Helman, 1990; Churchill, 2008; Woinarski *et al.*, 2014; Augusteyn *et al.*, 2018; Armstrong *et al.*, 2019). This taxon is also represented in the early Pleistocene deposit of Rackham's Roost, Riversleigh (Hand, 1996; Woodhead *et al.*, 2016), as well as many sites of Pleistocene and Holocene age around Australia (Molnar *et al.*, 1984). In Western Australia, fossil and subfossil bat material has been discovered in very few localities, though *M. gigas* is a conspicuous presence in numerous limestone caves in the south-west corner (reviews in Cook, 1960; Bridge, 1975; Baynes *et al.*, 1975; Molnar *et al.*, 1984; Armstrong & Anstee, 2000), and few of these caves are now used by bats of any species (Armstrong *et al.*, 2005). Megadermatid fossils have also been discovered further north on Barrow Island and the Monte Bello Islands off the Pilbara coast (Ken Aplin, unpublished observations).

More recently, a limestone deposit from Dingo Gap in the Kimberley region, north-west of Fitzroy Crossing (Fig. 1), has produced material from a range of fossil mammals, which includes at least three species of bat. One of these is clearly a megadermatid, which is described here as a new species. The other bat species are not sufficiently well represented for identification or formal description, but they do provide context for the occurrence of the megadermatid bones and teeth.

Methods

Scanning electron micrographs were taken with a Jeol JSM6060B microscope. Holotype and paratype material was examined and illustrated in comparison with a specimen of *M. gigas* from the CSIRO Australian National Wildlife Collection (ANWC), Canberra (CM568, male, collected from Mt Etna, Queensland), as well as material in the Western Australian Museum (WAM; three dentaries from *M. gigas* specimens M3415, M18284 and M18575; all from the Pilbara region of Western Australia). Descriptions are made in comparison with information in Hand (1985, 1995, 1996) and Hand *et al.* (1988). Measurements were made from SEM images using the software ImageJ (Rasband, 1997–2005; Abramoff *et al.*, 2004). Measurements of the newly described species made for direct comparison with *M. gigas* correspond to a subset of those in Hand (1985) and are numbered accordingly (Fig. 2). Additional measurements made for descriptive purposes are indicated by letters (Table 1). Higher level systematics follow Simmons & Cirranello (2020). Anatomical terminology follows Hand (1985), Hand *et al.* (1988), and Hand (1996).

Systematics

Chiroptera Blumenbach, 1779

Yinpterochiroptera Springer, Teeling, Madsen, Stanhope & de Jong, 2001

Rhinolophoidea Gray, 1825

Megadermatidae H. Allen, 1864

Macroderma Miller, 1906

Macroderma handae sp. nov. Aplin and Armstrong

urn:lsid:zoobank.org:act:018A744D-3AE6-44C0-988E-018C963EEE8E

Figs 3–8

Holotype. Fragment of left dentary containing a mostly intact M_2, broken P_4, M_1 and M_3, and alveoli of single-rooted P_2 and C_1 (WAM 2020.4.1; Figs 3A,B and 4A,C,E,G). **Paratypes**. A second fragment of left dentary with alveoli of incisors, C_1, P_2 and P_4, and first two molars (WAM 2020.4.2; Fig. 3D,E); a third fragment of left dentary containing a worn M_1 and one alveolus of M_2 (WAM 2020.4.3; Fig. 3C); palatal fragment of left maxilla with lingual alveoli of P^4 and M^1 (WAM 2020.4.4; Fig. 5B,C); fragment of right maxilla with alveoli of C^1 and P^4 (WAM 2020.4.5; Fig. 5A); right M^1 (WAM 2020.4.6; Fig. 6A,C); right M^2 fragment (WAM 2020.4.10; Fig. 6E); anterior portion of right C^1 (WAM 2020.4.7; Fig. 7A); right C^1 with broken paracone (principal cusp, *sensu* Hand, 1985; WAM 2020.4.9; Fig. 7C,D); left P_2 (WAM 2020.4.8; Fig. 8A,B,D); left M_3 in poor condition (WAM 2020.4.11; Fig. 4I); left P^4 with damaged paracone (principal cusp; WAM 2020.4.12; Fig. 8E–H). All type material is lodged in the Western Australian Museum.

Type locality, lithology, and age. Material was collected from a cemented accumulation of bone material that formed on the floor of a cave in a carbonate-rich stratigraphic sequence at Dingo Gap, Oscar Range, Kimberley region, Western Australia (17°40'S 125°13'E, Fig. 1). The location is part of the marginal reef slope and basinal facies of the northern face of the Oscar Range (Stephens & Sumner, 2003). This range forms the northern edge of the Canning Basin, and is the remnant of an Upper Devonian marine reef complex.

The bone accumulation was in a hard limestone matrix and consisted of teeth and small bone fragments of mammals, particularly rodents (Muridae: Hydromyini (*sensu* Smissen & Rowe, 2018); *Rattus* was absent). Further details of the fauna in this collection are not yet available. It is more likely to be an accumulation from a cave floor beneath a megadermatid bat roost site rather than a pellet accumulation from an owl given that larger jaw fragments were absent. Dental material from other bats was also present, including an unknown species of bat (Fig. 9A–D), canines from an emballonurid (probably *Taphozous* sp.; Fig. 9E–L), and a lower row of molars from an unidentified vespertilionid (Fig. 9M,N). Given the absence of *Rattus*, which is thought to have reached Australia by at least the mid-Pleistocene (Rowe *et al.*, 2019), the material is aged tentatively as Pliocene or early Pleistocene.

Diagnosis. Referred to the genus *Macroderma* Miller, 1906 on the basis of the large size of the $M^{1–2}$ (within the lower part of the size range of *M. gigas* and *M. koppa*; Table 1; cf. Hand, 1995: 52), the M^1 with elongated heel, and markedly lingually displaced mesostyle (cf. *Megaderma richardsi*; Hand, 1995: 66); $M_{1–3}$ paracristid (*sensu* Hand, 1995, 1996; = protocristid *sensu* Hand, 1985, who used both terms) longer than metacristid; $M_{1–3}$ reduced metaconid contribution to the cristid obliqua; $M_{1–3}$ robust and continuous anterior, labial (= buccal) and posterior cingula (see Hand, 1996: 373).

Compared with *Macroderma gigas*—Maxilla fenestrated (Fig. 5B,C), but not to the degree seen in *M. gigas* (cf. Hand, 1985: 31); anterior part of dentary thickened, though relatively gracile compared with that of *M. gigas* (dentary depth below M_2 protoconid less in *M. handae*; Table 1; Fig. 3A,F); most molar measurements smaller than the average for *M. gigas*, or within the lower part of the size range (Table 1); the shape of the M^1 protofossa (whose edges are defined by the preprotocrista and postprotocrista) is rounded rather than triangular (Fig. 6A–D); M_2 paraconid lower, and protruding less anteriorly past the protoconid (trigonid less expanded anteriorly than in *M. gigas*); M_2 protoconid relatively high and of proportionally greater area within the trigonid (more than half in occlusal view (Fig. 4A,B); and M_2 talonid proportionally larger with respect to the trigonid (Fig. 4A,B). No protostyle cusp on P^4, which is obvious in *M. gigas* (Fig. 8E,F).

Compared with *M. koppa* (see Hand *et al.*, 1988: 344–346)—Anterior upper tooth row relatively shorter in *M. handae*, alveoli of C^1 and P^4 indicating overlap of crowns

Table 1. Measurements (mm; Fig. 2) of the holotype dentary and M_2 (WAM 2020.4.1), and the paratypes M^1 (WAM 2020.4.6) and C^1 (WAM 2020.4.7) of *Macroderma handae* sp. nov., in comparison with *M. gigas* and *M. koppa* (values and character numbers are from Hand, 1985: 23,25; Hand *et al.*, 1988: 349; mean and range in parentheses; RR indicates measurements from *M. gigas* in Rackham's Roost, see Hand, 1996: 370; letters in the first column represent measurements made in the present study only; * measurement from paratype WAM 2020.4.2).

	holotype dentary and M_2	*M. handae*	*M. gigas*	*M. koppa*
3	Dentary depth below M_2 protoconid	3.5, 3.42*	3.92 (3.40–4.90) RR: 3.45	4.2 (4.4–4.5)
10	M_2 length (sum measurements 14 + 15)	3.21	3.78 (3.41–4.17) RR: 3.27	4.2 (3.9–4.1)
14	M_2 trigonid length	1.73	2.41 (1.91–2.79) RR: 2.10	2.5 (2.3–2.5)
15	M_2 talonid length	1.48	1.41 (1.00–1.88) RR: 1.19	1.6 (1.3–1.6)
21	M_2 trigonid width	2.36	2.38 (2.05–2.68)	2.8 (2.4–2.6)
22	M_2 talonid width	2.16	2.31 (1.86–2.85)	2.6 (2.2–2.5)
27	M_2 paracristid length	1.44	1.72 (1.38–1.92)	—
28	M_2 metacristid length	1.04	1.25 (0.98–1.65)	—
A	M_2 protoconid height (not illustrated)	3.19	—	—
B	Mental foramen width (not illustrated)	0.53, 0.55	—	—
	paratypes M^1 and C^1	***M. handae***	***M. gigas***	***M. koppa***
14	M^1 labial (buccal) length	3.53	3.93 (3.36–4.40) RR: 3.36, 3.52	4.1 (4.0–4.2)
18	M^1 lingual length	3.13	4.24 (3.60–4.76) RR: 3.59, 3.85	4.0
21	M^1 width	3.95	4.15 (3.65–4.63) RR: 3.43, 3.94	4.4 (4.1–4.3)
25	M^1 metacone apex to metastyle	2.15	2.73 (2.36–2.88)	—
28	M^1 paracone to heel	2.43	3.20 (2.29–3.66)	—
30	M^1 heel inflexions	1.49	2.34 (1.84–3.54)	—
32	M^1 length through protocone	1.70	2.44 (2.08–2.90)	—
C	M^1 protofossa width	1.20	—	—
D	M^1 heel width	1.37	—	—
E	C^1 height (not illustrated)	4.29	—	—

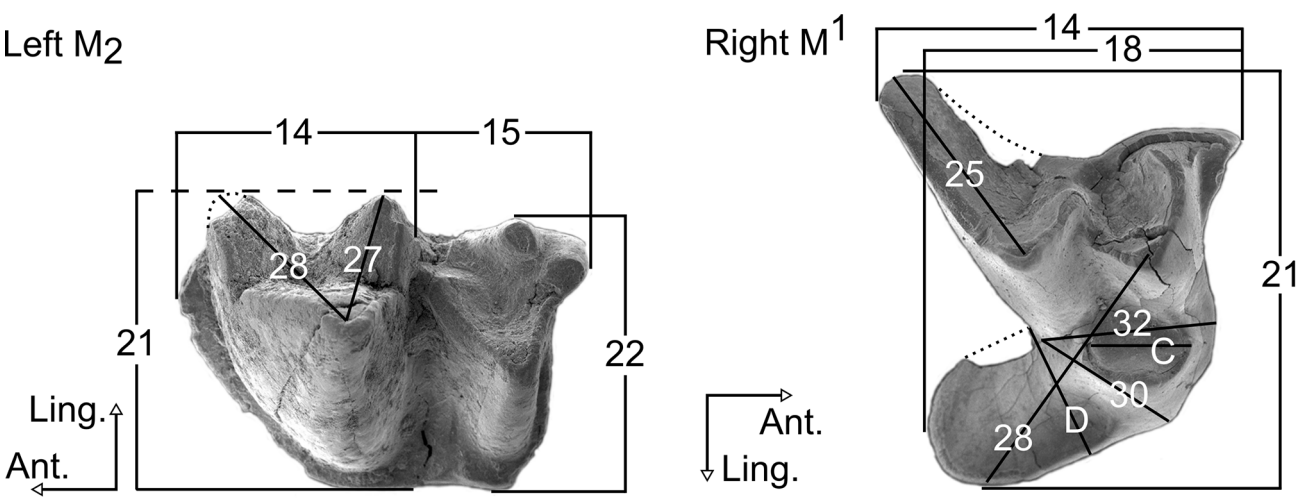

Figure 2. Dental measurements taken from the left M_2 and the right M^1, based on Hand (1985).

(Fig. 5A; cf. Hand *et al.*, 1988: 345, fig. 2b,c); the shape of the M^1 protofossa (with edges defined by the preprotocrista and postprotocrista) is rounded rather than triangular; molar measurements smaller than the values for *M. koppa* (Table 1; cf. Hand *et al.*, 1988: 349); anterior part of dentary relatively gracile compared with that of *M. koppa* (dentary depth below M_2 protoconid less in *M. handae*; Table 1); M_2 paraconid relatively low, and protruding less anteriorly past the protoconid due to anterior compression of the trigonid (Fig. 4C,E; cf. Hand *et al.*, 1988: 345, fig. 2a); M_2 protoconid relatively high and of proportionally greater area within the trigonid (more than half in occlusal view; Fig. 4A); entoconid smaller than hypoconulid (Fig. 4E,G; cf. Hand *et al.*, 1988: 345, fig. 2a); the P_2 is of a similar shape in both species (Fig. 8A,B,D; cf. Hand *et al.*, 1988: 345, fig. 2a).

Compared with *M. malugara* Hand, 1996—P^2 absent in *M. handae*; slightly smaller size of M^1 and M_2 (Table 1; cf. Hand, 1996: 368); the shape of the M^1 protofossa (whose edges are defined by the preprotocrista and postprotocrista) is rounded rather than triangular; M_2 paraconid relatively low, and protruding less anteriorly past the protoconid due to anterior compression of the trigonid (Fig. 4A,C,E; cf. Hand, 1996: 366–367, pl. 48k–m); M_2 protoconid relatively high and of proportionally greater area of the trigonid (more than

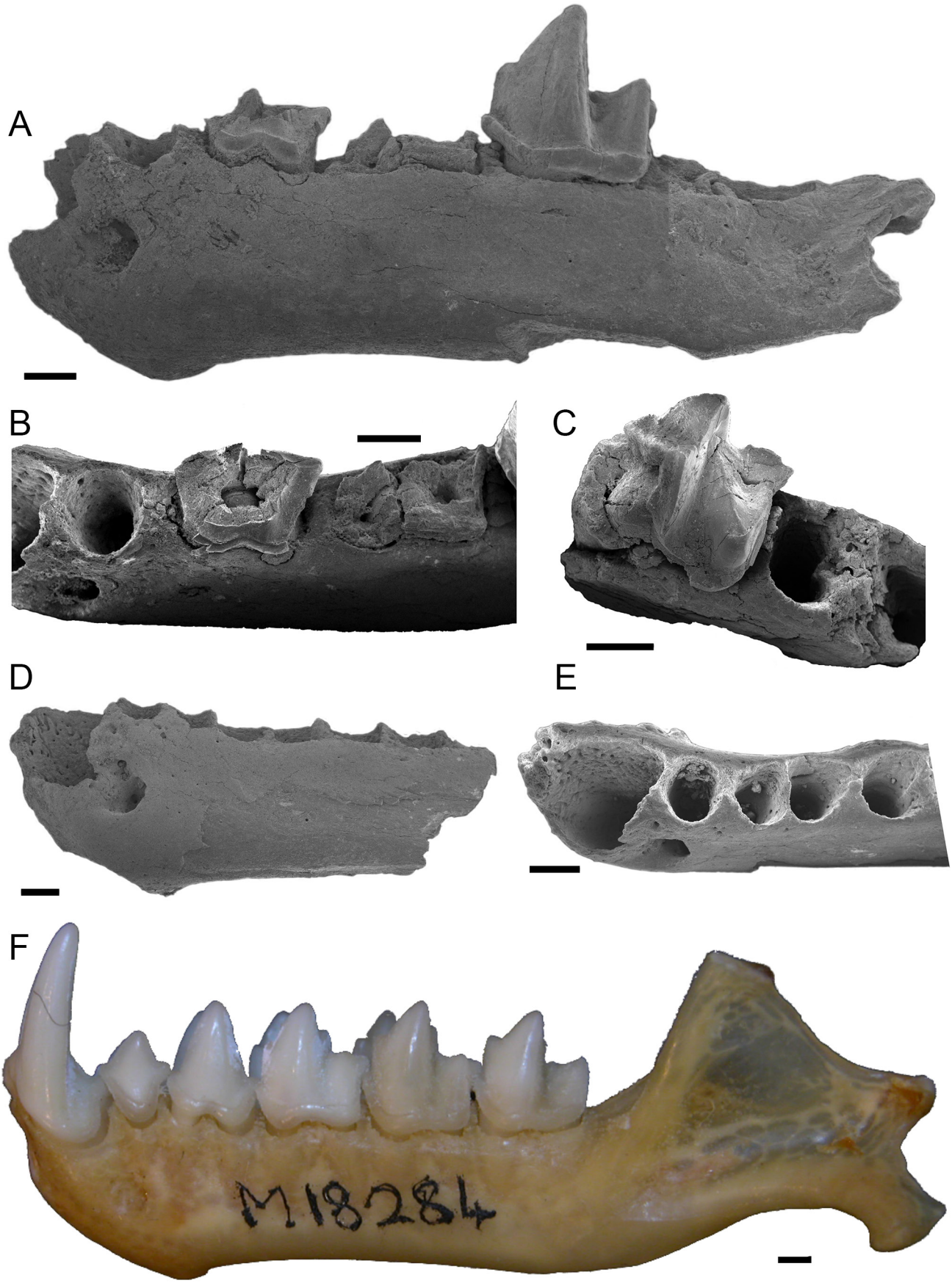

Figure 3. Scanning electron micrographs of holotype and paratype material of *Macroderma handae* sp. nov. (*A*) lateral view of the left dentary of holotype WAM 2020.4.1 with mostly intact M_2, broken P_4, M_1 and M_3, and alveoli of single-rooted P_2 and C_1; (*B*) occlusal view of the holotype WAM 2020.4.1 anterior to the M_2; (*C*) occlusal view of a fragment of left dentary, paratype WAM 2020.4.3; (*D, E*) lateral and occlusal view of a fragment of left dentary, paratype WAM 2020.4.2; (*F*) digital photograph of the left dentary of *M. gigas* WAM M18284. Scale bars 1 mm.

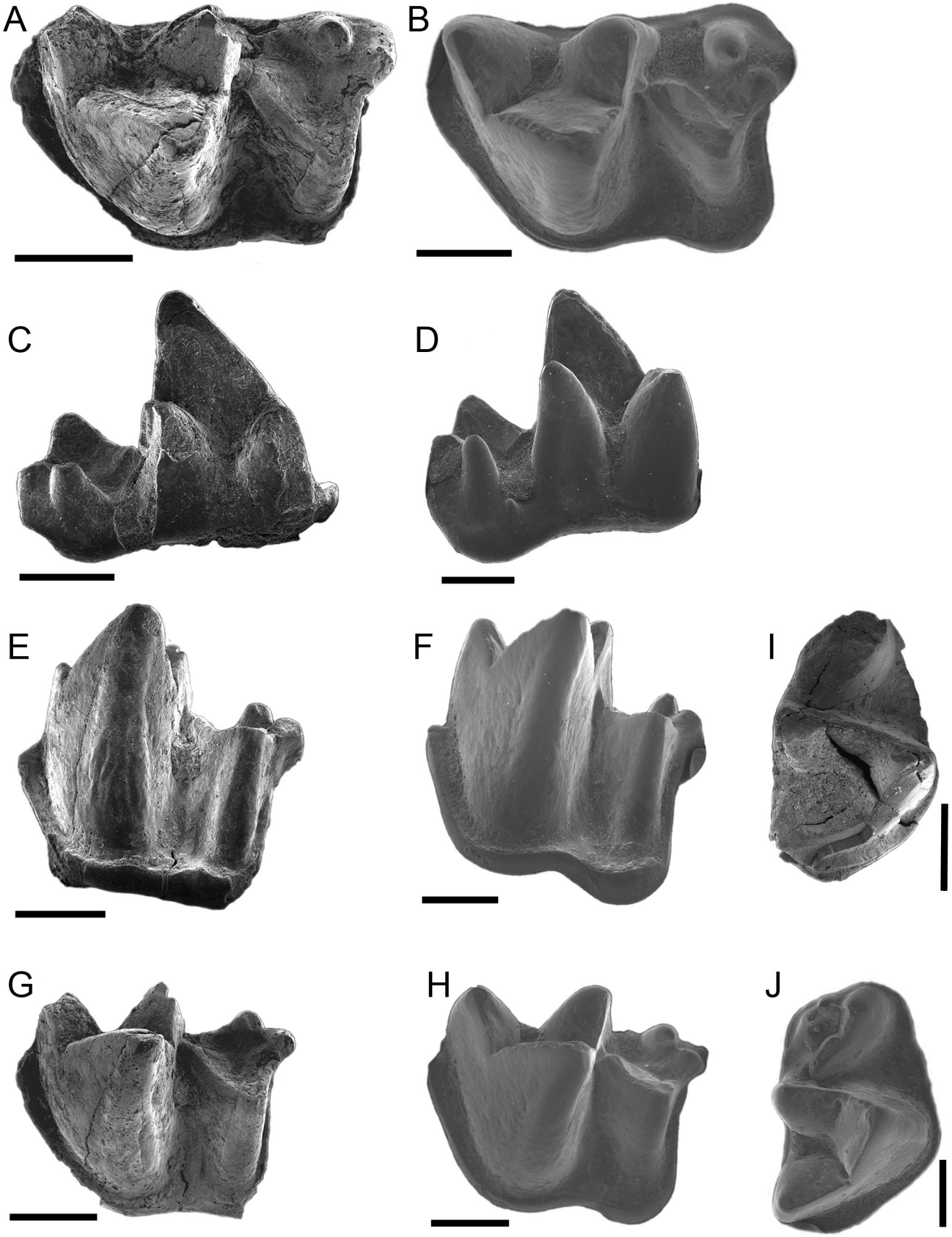

Figure 4. Scanning electron micrographs of holotype and paratype material of *Macroderma handae* sp. nov. (*A, C, E, G*) occlusal, lingual, labial, and labial-oblique views of the left M_2 from the holotype WAM 2020.4.1; (*B, D, F, H*) corresponding views of the left M_2 of *M. gigas* ANWC CM568; (*I*) occlusal view of left M_3, paratype WAM 2020.4.11; (*J*) left M_3 of *M. gigas* ANWC CM568. Scale bars 1 mm.

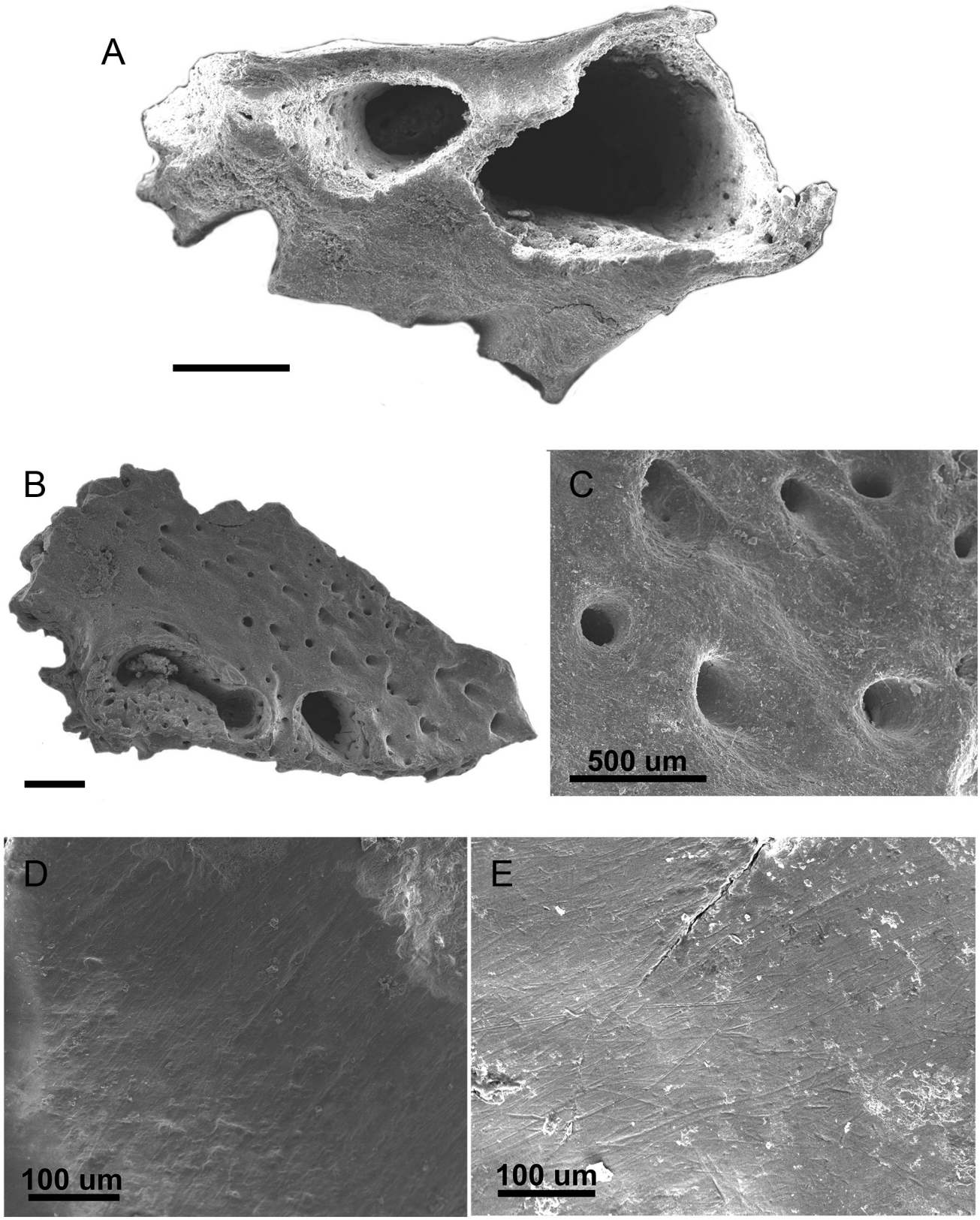

Figure 5. Scanning electron micrographs of paratype material of *Macroderma handae* sp. nov. (*A*) fragment of the right maxilla with alveoli of the C^1 and P^4, paratype WAM 2020.4.5; (*B*) palatal fragment of left maxilla with lingual alveoli of P^4 and M^1, paratype WAM 2020.4.4; (*C*) detail of the blood vessel fenestrations in paratype WAM 2020.4.4; (*D*) probable wear striations on the M_3, paratype WAM 2020.4.11; (*E*) wear striations from *M. gigas* ANWC CM568. Scale bars 1 mm, except where indicated otherwise.

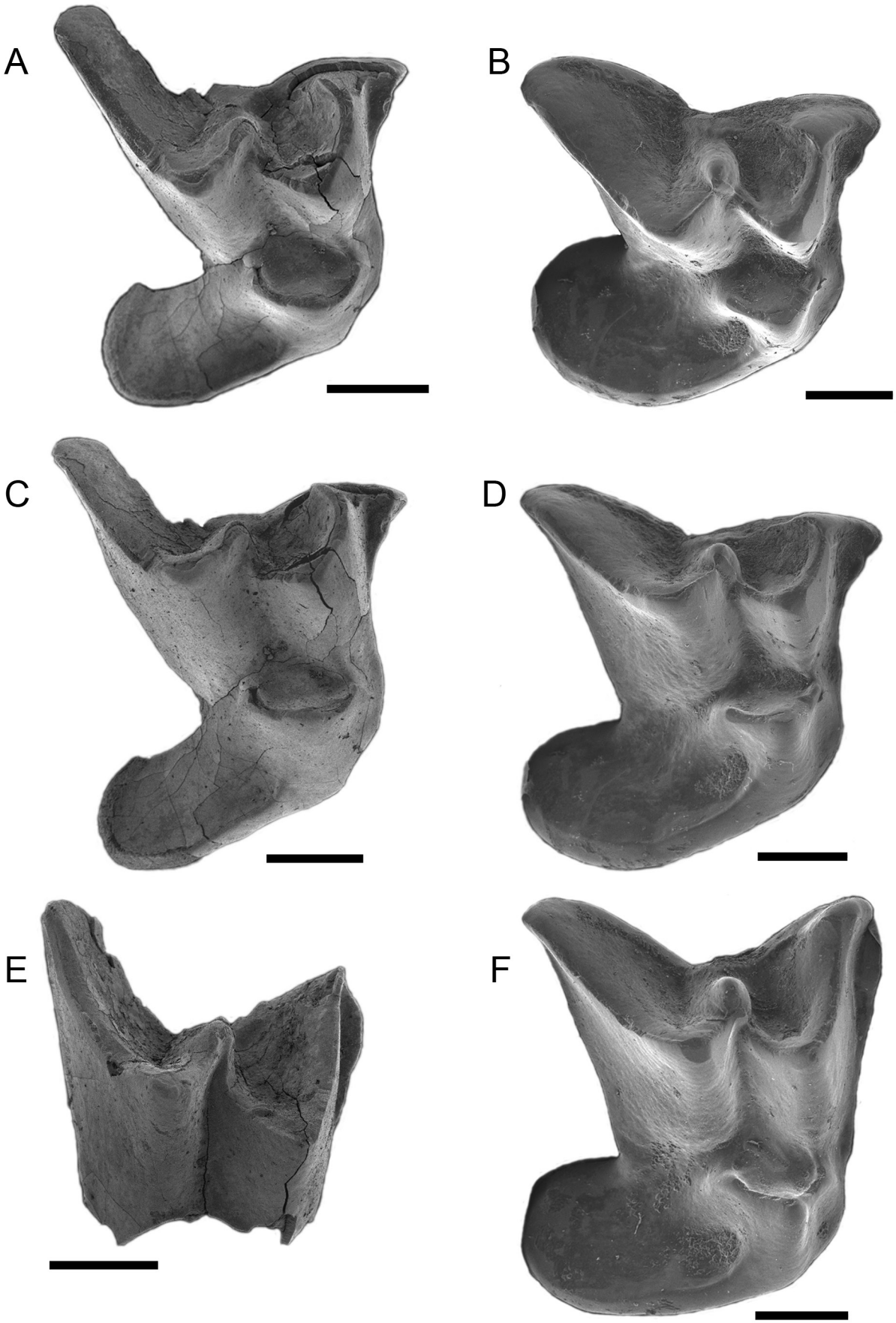

Figure 6. Scanning electron micrographs of paratype material of *Macroderma handae* sp. nov. (*A, C*) occlusal-oblique views of a right M^1, paratype WAM 2020.4.6; (*B, D*) corresponding views of the right M^1 of *M. gigas* ANWC CM568; (*E*) occlusal view of a fragment of a right M^2, paratype WAM 2020.4.10; (*F*) corresponding view of the right M^2 of *M. gigas* ANWC CM568. Scale bars 1 mm.

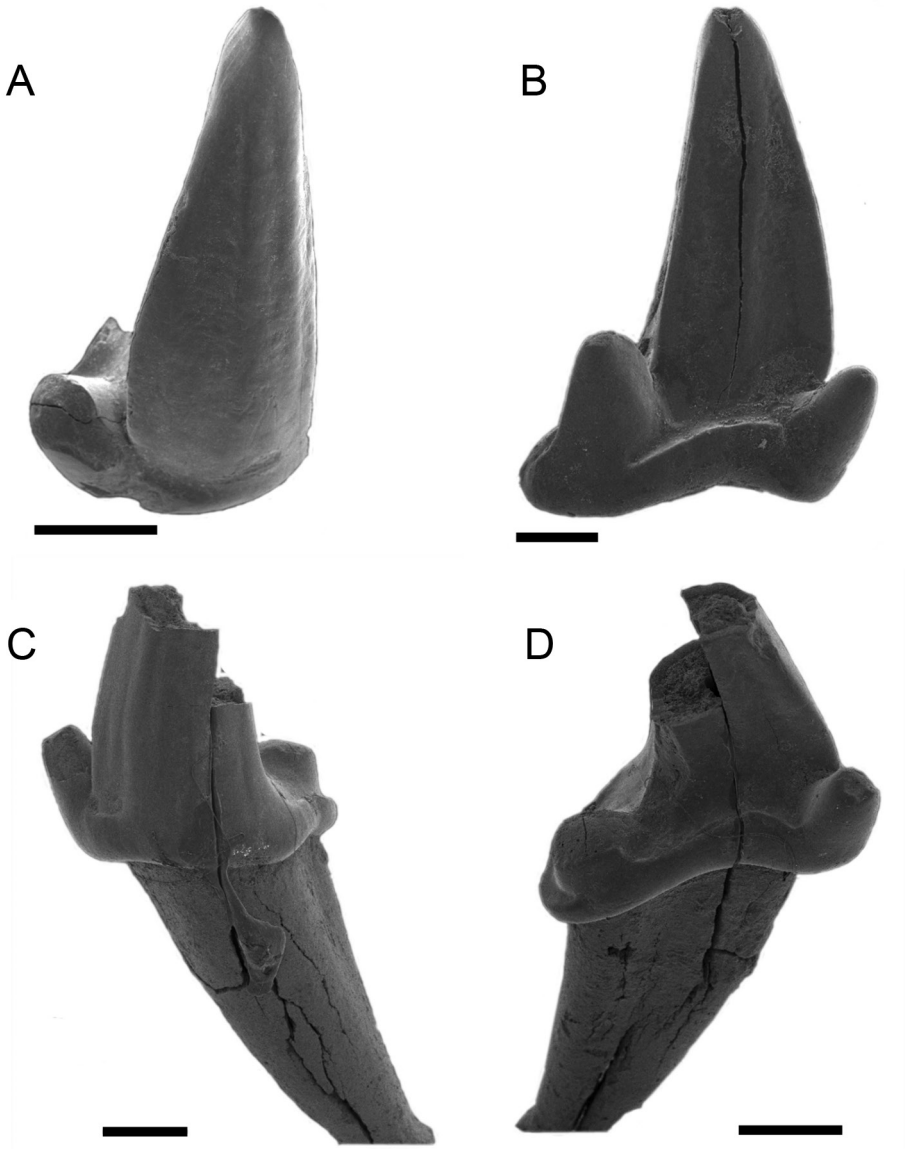

Figure 7. Scanning electron micrographs of paratype material of *Macroderma handae* sp. nov. (*A*) anterior half of a right C^1, paratype WAM 2020.4.7; (*B*) lingual view of a right C^1 of *M. gigas* ANWC CM568; (*C, D*) labial and lingual views of a right C^1 with a damaged paracone, paratype WAM 2020.4.9. Scale bars 1 mm.

half in occlusal view; Fig. 4A; cf. Hand, 1996: 366–367, pl. 48m); greater development of M_2 hypoconulid (Fig. 4A; cf. Hand, 1996: 366–367, pl. 48m).

Compared with *M. godthelpi* Hand, 1985—C^1 and M^1 and M_2 slightly larger in size in *M. handae*, and M_2 with greater protoconid height (Table 1; cf. measurements in Hand, 1985: 8–9; see also Sigé *et al.*, 1982 for measurement key); taller and more robust C^1 (Table 1*E*; Fig. 7A,C,D; cf. Hand, 1985: 9,12, fig. 5a,b); loss of P^2; proportionally greater contribution of the cingulum to the height of the P_2 (cf. Hand, 1985: 13, fig. 6c); M_2 paraconid relatively low, and protruding less anteriorly past the protoconid due to anterior compression of the trigonid (Fig. 4A,C,E; cf. Hand, 1985: 11, fig. 4a,b,c); M_2 protoconid relatively high and of proportionally greater area of the trigonid (more than half in occlusal view; Fig. 4A; cf. Hand, 1985: 11, fig. 4c).

Description. The anterior part of the dentary is thickened, though relatively gracile and shallower in depth compared to *M. koppa* and *M. gigas*, with likely two lower incisors per side (paratype WAM 2020.4.2; anterior detail not shown in Fig. 3A,B,D,E). Two premolars are present—P_2 and P_4, in addition to the $M_{1–2}$ (Fig. 3A,B), and the M_3 (Fig. 4I).

There is marked extension posterolingually of the C_1, similar to *M. gigas* (Fig. 7A–D). The P_2 has a proportionally large cingulum, as can be seen in occlusal view, which gives the tooth the appearance of a "witches hat" when viewed from either the labial or lingual side (Fig. 8A,B,D).

The M_1 is shorter than, or equal in length to, the tall-crowned M_2 (Fig. 3A). The paracristid of the M_2 is longer than the metacristid (Fig. 4A). There is relatively little contribution of the M_2 metaconid to the cristid obliqua (Fig. 4A). The M_2 hypoconulid is situated posteriorly (Fig. 4A). The anterior, labial, and posterior cingula are robust and continuous (Fig. 4A,E,G). There is no development of the entostylid (Fig. 4A).

The maxilla is rugose and fenestrated, with grooves of blood vessels along the surface (Fig. 5B,C). The condition of the infraorbital foramen (a key feature separating *M.*

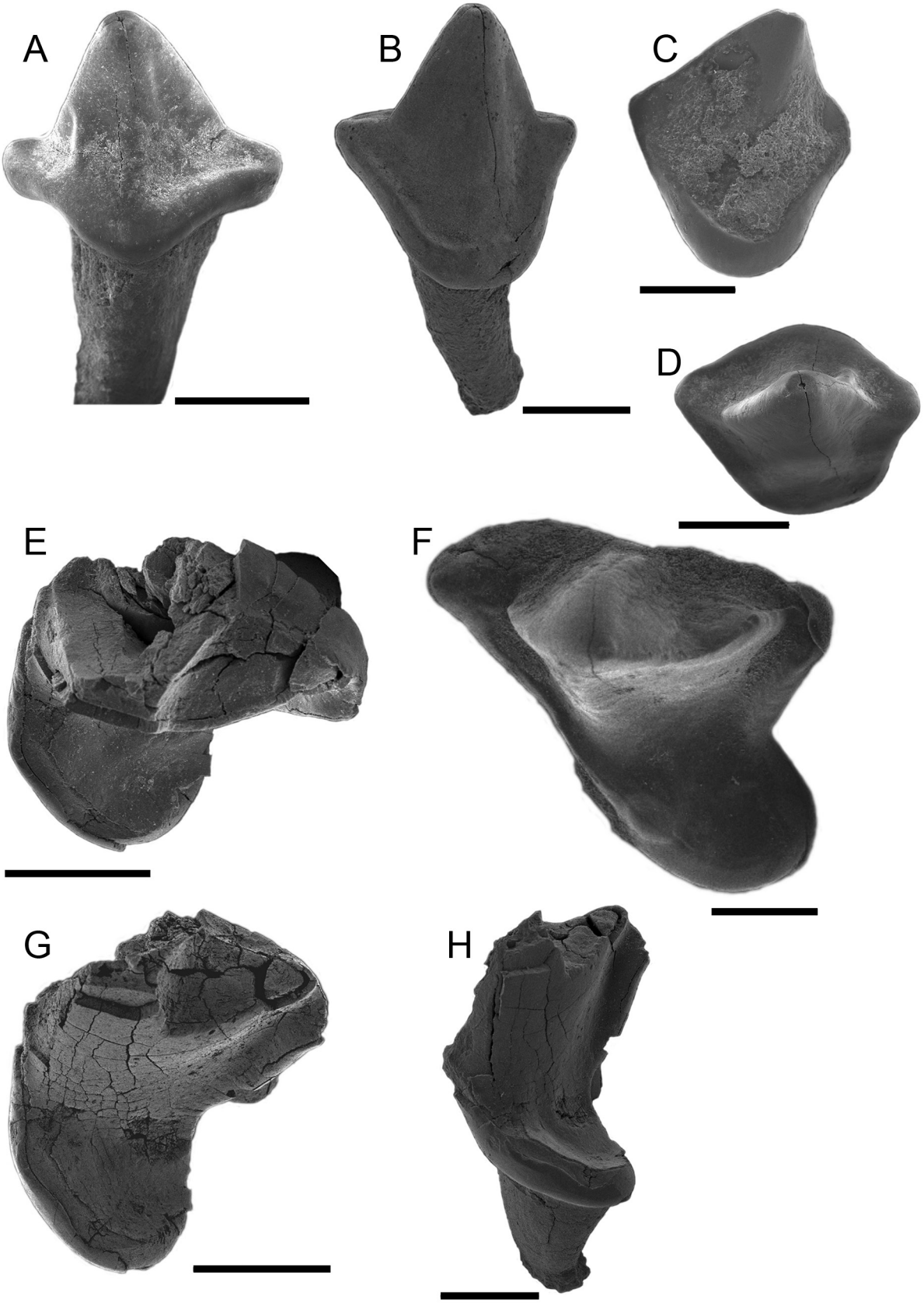

Figure 8. Scanning electron micrographs of paratype material of *Macroderma handae* sp. nov. (*A, B, D*) lingual, labial and occlusal views of a left P_2, paratype WAM 2020.4.8; (*C*) labial view of the left P_2 of *M. gigas* ANWC CM568; (*E, G, H*) occlusal, lingual-oblique, and posterior views of a damaged left P^4, paratype WAM 2020.4.12; (*F*) occlusal view of a left P^4 of *M. gigas* ANWC CM568. Scale bars 1 mm.

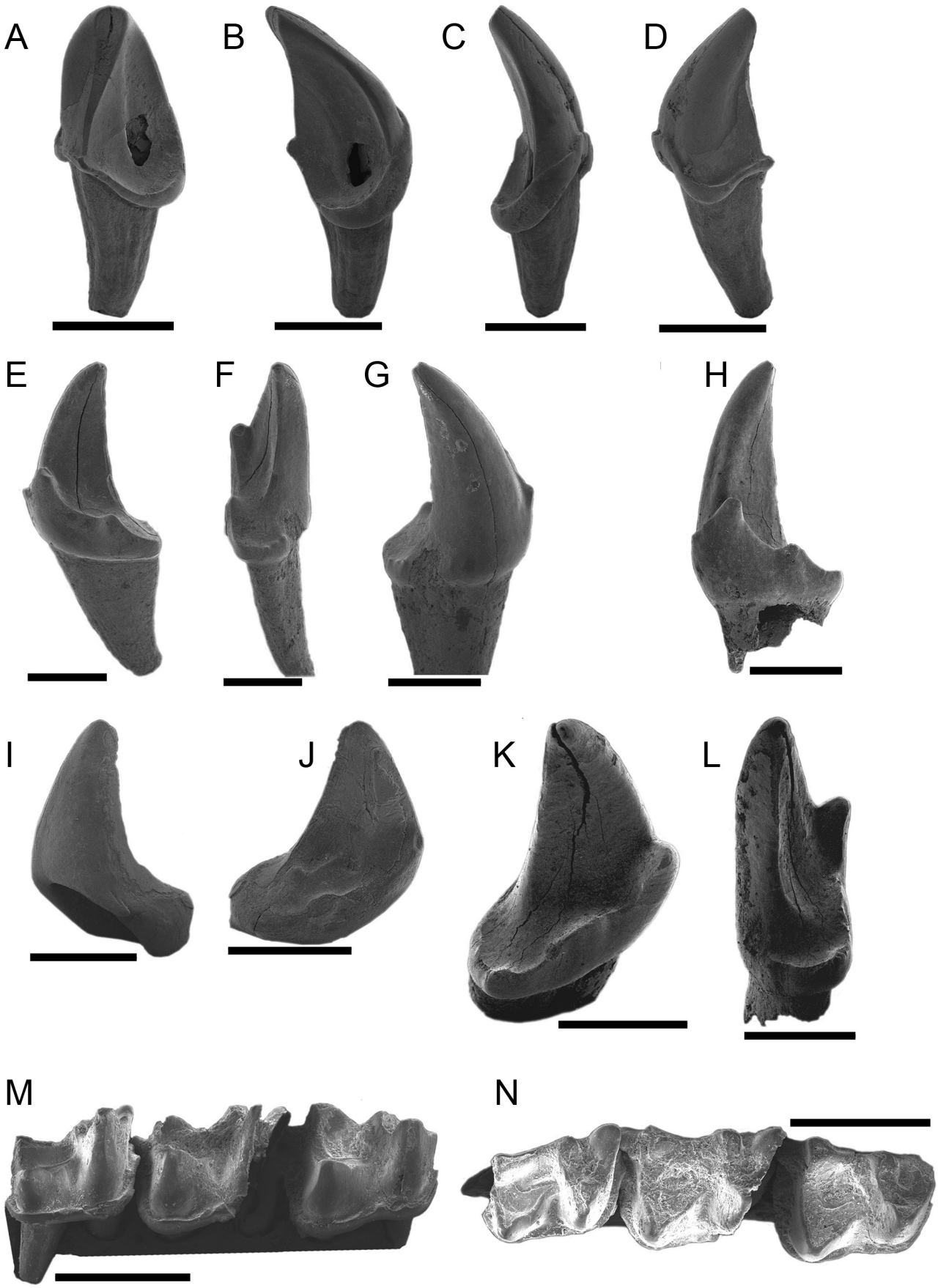

Figure 9. Scanning electron micrographs of other unidentified and undescribed bat material recovered from the same deposit at Dingo Gap. (*A–D*) WAM 2020.4.13; (*E–G*) right C_1 of an emballonurid, WAM 2020.4.14; (*H*) right C_1 of an emballonurid, WAM 2020.4.15; (*I, J*) left C_1 of an emballonurid, WAM 2020.4.16; (*K, L*) left C_1 of an emballonurid, WAM 2020.4.17; (*M, N*) lingual and occlusal views of a fragment of dentary of a vespertilionid containing M_1–M_3 (M_1 is on the right in both views), WAM 2020.4.18. Scale bars 1 mm.

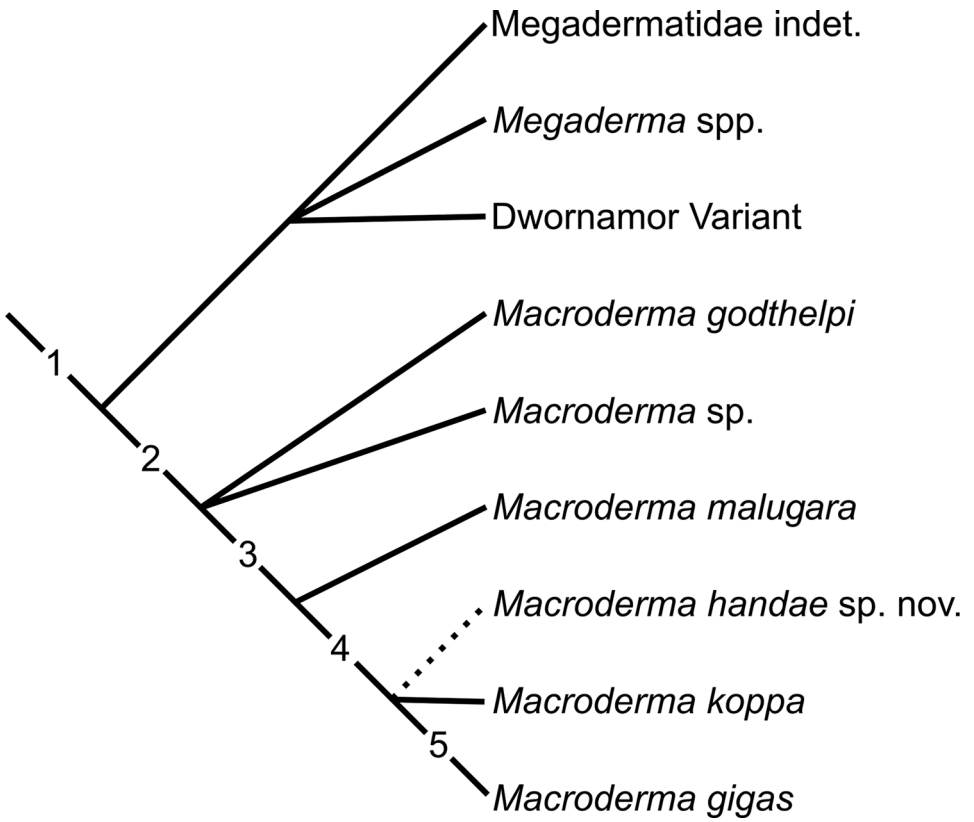

Figure 10. Inferred relative phylogenetic position of *Macroderma handae* sp. nov. based on observable synapomorphic features (modified after Hand, 1996; numbers indicate the development of potential apomorphic character states, as detailed in that reference).

koppa [two foramina] and *M. gigas* [one foramen]; Fig. 5A) cannot be observed.

The P^2 is absent, as indicated by the absence of an alveolus between those of the canine and P^4 (paratype WAM 2020.4.5; Fig. 5A). The alveolus of C^1 and anterobuccal/anterolabial alveolus of P^4 indicate that the crowns of these teeth overlapped in the tooth row (Fig. 5A). The heel of the P^4 is broad, and the posterior edge is at right angles to the paracone (it is angled close to 45° lingually in *M. gigas*; Fig. 8E–H). There is no protostyle cusp, which is obvious in *M. gigas* (Fig. 8E,F).

The M^1 has a broad labial (buccal, *sensu* Hand, 1996) shelf, though narrower than that of *M. gigas* (Fig. 6A,B), and a markedly lingually displaced mesostyle (cf. *Megaderma richardsi*; Hand, 1995). The preprotocrista and postprotocrista are curved, giving the protofossa a rounded shape, which contrasts with the more triangular form of other *Macroderma* species (Hand *et al.*, 1988: 345, fig. 2c; Hand, 1985: 10, fig. 3c, 1996: 366–367, pl. 48d), and also *Megaderma richardsi* (Hand, 1995: pl. 1b,c). Both the M^1 and M^2 have tall crowns, and appear to be slightly compressed anteroposteriorly relative to *Macroderma gigas* (Fig. 6A–F).

Unidirectional wear striations are observable on the left M_3, which resemble those found on the teeth of the predatory *M. gigas* that crush the bones of prey (Fig. 5D,E).

Etymology. Named in honour of Professor Suzanne ("Sue") J. Hand of the University of New South Wales, in recognition of her previous extensive work on fossils of this family, and her extraordinary, sustained, and ongoing work on fossils that has helped piece together the rich history of the Australasian mammal fauna.

Discussion

Phylogenetic relationships

The phylogenetic position of *Macroderma handae* relative to most megadermatids can be estimated based on the presence of various synapomorphies that characterize subclades within the family (character sets 1–5 listed in Hand, 1996: 373) (Fig. 10). It displays the following apomorphic conditions: (*a*) Characterizing it as part of the *Megaderma–Macroderma* clade: M_1 shorter than or equal in length to M_2. (*b*) Distinguishing it from the *Megaderma* clade: M^1 with elongated heel, and markedly lingually displaced mesostyle (cf. *Megaderma richardsi*; Hand, 1995); in the M_2: the paracristid longer than metacristid, reduced metaconid contribution to the cristid obliqua; robust, continuous anterior, labial and posterior cingula. (*c*) Distinguishing it from *Macroderma godthelpi*: large-sized, tall-crowned teeth; M_2 with robust and broad anterior cingulum. (*d*) Distinguishing it from *M. malugara*: P^2 absent; C_1 markedly posterolingually-extended; M_{1-2} larger and more posteriorly-situated hypoconulid; and preentocristid further reduced. The phylogenetic position of *M. handae* relative to *M. koppa* and *M. gigas* could not, however, be determined unambiguously based on the material from Dingo Gap because the condition of the infraorbital foramen (one or two foramina) and some other diagnostic features could not be observed.

Australian Pliocene megadermatid diversity

The new species *M. handae* represents the second Pliocene species of *Macroderma* discovered to date, together with

M. koppa. The age of the Big Sink Site of Wellington Caves in New South Wales has also been estimated as Pliocene, though it has not been dated other than on the basis of biocorrelation with better-dated faunas (reviews in Hand, 1996; Dawson *et al.*, 1999), and the inferred plesiomorphic condition of *M. koppa* (Dawson *et al.*, 1999: 284). Both sites lack *Rattus* material, though they have representatives of the Old Endemic murid radiation (Hydromyini, *sensu* Smissen & Rowe, 2018), so their likely age is at least somewhere between the first Australian murid radiations and the invasion of *Rattus* (Aplin, 2006; Rowe *et al.*, 2019). The species *M. handae* and *M. koppa* might have been contemporaneous, or alternatively they could have arisen at slightly different ages sometime from the late Miocene to early Pliocene. While *M. handae* appears slightly smaller on the basis of a few molar measurements, it is not markedly so. Thus, it might have been an earlier or allopatric taxon. A proposed common name for *M. handae* is the Kimberley False Vampire Bat.

Chiropteran assemblage

Several other bat species were recovered from the same assemblage that contained *M. handae* (Fig. 9). The lack of molars, or those in an unbroken condition, precluded identification to species, or species description. But on the basis of canine morphology (the position of cingular cusps), an emballonurid species, most likely representing the genus *Taphozous*, is present. A small vespertilionid species was also present. Based on the wear striations on the M_3 of *M. handae* (Fig. 5D), probably derived from crushing the bones of vertebrates, these smaller bat species might well have been prey, as well as co-inhabitants of the roost. Body parts of the species *Taphozous georgianus*, *Rhinonicteris aurantia* and *Vespadelus finlaysoni* have all been observed in the prey accumulations of modern *M. gigas* in the Pilbara region of Western Australia and Northern Territory (Churchill, 2008; K. N. Armstrong personal observations).

Acknowledgements. The authors are grateful to the Kyoto University Museum for support and use of facilities; to Hidetoshi Nagamasu for help with the SEM; the Western Australian Museum and the Australian National Wildlife Collection for the loan of material; Alexander Baynes of the Western Australian Museum for information on the collection and careful editing of the manuscript; and to Robin Beck, Gilbert Price, and Sue Hand, for helpful review comments that resulted in a much-improved text. KPA acknowledges the support of the Kyoto University Museum, which hosted him as a visiting professor; and KNA gratefully acknowledges the support of a JSPS Postdoctoral Fellowship for Foreign Researchers while at the Kyoto University Museum. Ken Aplin is a posthumous author on this publication. He collected and discovered the material described herein, designed the study, took the images together with KNA, and made numerous contributions and comments as the earlier versions of the manuscript were drafted. Some details about Ken's Dingo Gap collection are unfortunately not available.

References

Abramoff, M. D., P. J. Magelhaes, and S. J. Ram. 2004. Image processing with ImageJ. *Biophotonics International* 11: 36–42.

Aplin, K. P. 2006. Ten million years of rodent evolution in Australasia: phylogenetic evidence and a speculative historical biogeography. In *Evolution and Biogeography of Australasian Vertebrates*, ed. J. R. Merrick, M. Archer, G. M. Hickey, and M. S. Y. Lee, pp. 707–744. Oatlands, Sydney: Auscipub.

Archer, M., D. A. Arena, M. Bassarova, R. M. Beck, K. Black, W. E. Boles, P. Brewer, B. N. Cooke, K. Crosby, A. Gillespie, H. Godthelp, S. J. Hand, B. P. Kear, J. Louys, A. Morrell, J. Muirhead, K. K. Roberts, J. D. Scanlon, K. J. Travouillon, and S. Wroe. 2006. Current status of species-level representation in faunas from selected fossil localities in the Riversleigh World Heritage Area, northwestern Queensland. *Alcheringa* 30: 1–17. https://doi.org/10.1080/03115510608619570

Armstrong, K. N., R. Brown, and P. Armstrong. 2005. The status of bat roosts in caves in the south west of Western Australia, with a focus on Quininup Lake Cave. *The Western Australian Naturalist* 25: 41–56.

Armstrong, K. N., and S. D. Anstee. 2000. The ghost bat in the Pilbara: 100 years on. *Australian Mammalogy* 22: 93–101. https://doi.org/10.1071/AM00093

Armstrong, K. N., J. C. Z. Woinarski, N. M. Hanrahan, and A. A. Burbidge. 2019. *Macroderma gigas*. The IUCN Red List of Threatened Species 2019: e.T12590A22027714. https://doi.org/10.2305/IUCN.UK.2019-3.RLTS.T12590A22027714.en

Augusteyn, J., J. Hughes, G. Armstrong, K. Real, and C. Pacioni. 2018. Tracking and tracing central Queensland's *Macroderma*—determining the size of the Mount Etna ghost bat population and potential threats. *Australian Mammalogy* 40: 243–253. https://doi.org/10.1071/AM16010

Bate, D. M. A. 1937. New Pleistocene mammals from Palestine. *Annals and Magazine of Natural History* (10)20: 397–400. https://doi.org/10.1080/00222933708655355

Baynes, A., D. Merrilees, and J. K. Porter. 1976. Mammal remains from the upper levels of a late Pleistocene deposit in Devil's Lair, Western Australia. *Journal of the Royal Society of Western Australia* 58: 97–126.

Bridge, P. 1975. Paleo-distribution of *Macroderma gigas* in the southwest of Western Australia. *Helictite* 13: 34–36.

Churchill, S. K. 2008. *Australian Bats,* 2nd edition. Crows Nest, N.S.W.: Allen and Unwin.

Churchill, S. K., and P. M. Helman. 1990. Distribution of the ghost bat, *Macroderma gigas*, (Chiroptera: Megadermatidae) in central and South Australia. *Australian Mammalogy* 13: 149–56.

Cook, D. L. 1960. Some mammal remains found in caves near Margaret River. *The Western Australian Naturalist* 7: 107–108.

Dawson, L., J. Muirhead, and S. Wroe. 1999. The Big Sink Local Fauna: a lower Pliocene mammalian fauna from the Wellington Caves complex, Wellington, New South Wales. *Records of the Western Australian Museum* supplement no. 57: 265–290.

Foley N. M., V. D. Thong, P. Soisook, S. M. Goodman, K. N. Armstrong, D. Jacobs, S. J. Peuchmaille, and E. C. Teeling. 2015. How and why overcome the impediments to resolution: lessons from rhinolophid and hipposiderid bats. *Molecular Biology and Evolution* 32: 313–333. https://doi.org/10.1093/molbev/msu329

Gunnell G. F., E. L. Simons, and E. R. Seiffert. 2008. New bats (Mammalia: Chiroptera) from the late Eocene and early Oligocene, Fayum Depression, Egypt. *Journal of Vertebrate Paleontology* 28: 1–11. https://doi.org/10.1671/0272-4634(2008)28[1:NBMCFT]2.0.CO;2

Hand, S. J. 1985. New Miocene megadermatids (Chiroptera: Megadermatidae) from Australia, with comments on megadermatid phylogenetics. *Australian Mammalogy* 8: 5–43.

Hand, S. J. 1990. First Tertiary molossid (Microchiroptera: Molossidae) from Australia: its phylogenetic and biogeographic implications. *Memoirs of the Queensland Museum* 28: 175–192.

Hand, S. J. 1995. First record of the genus *Megaderma* Geoffroy, 1810 (Microchiroptera: Megadermatidae) from Australia. *Palaeovertebrata* 24: 47–66.

Hand, S. J. 1996. New Miocene and Pliocene megadermatids (Mammalia, Microchiroptera) from Australia, with comments on broader aspects of megadermatid evolution. *Geobios* 29: 365–377.
https://doi.org/10.1016/S0016-6995(96)80038-6

Hand, S. J. 1997a. New Miocene leaf-nosed bats (Microchiroptera: Hipposideridae) from Riversleigh, northwestern Queensland. *Memoirs of the Queensland Museum* 41: 335–349.

Hand, S. J. 1997b. *Miophyllorhina riversleighensis* gen. et sp. nov., a Miocene leaf-nosed bat (Microchiroptera: Hipposideridae) from Riversleigh, Queensland. *Memoirs of the Queensland Museum* 41: 351–354.

Hand, S. 1998a. *Riversleigha williamsi* gen. et sp. nov., a large Miocene hipposiderid (Microchiroptera) from Riversleigh, Queensland. *Alcheringa* 22: 259–276.
https://doi.org/10.1080/03115519808619204

Hand, S. 1998b. *Xenorhinos*, a new genus of old world leaf-nosed bats (Microchiroptera: Hipposideridae) from the Australian Miocene. *Journal of Vertebrate Paleontology* 18: 430–439.
https://doi.org/10.1080/02724634.1998.10011070

Hand, S. J., and M. Archer. 2005. A new hipposiderid genus (Microchiroptera) from an early Miocene bat community in Australia. *Palaeontology* 48: 1–13.
https://doi.org/10.1111/j.1475-4983.2005.00444.x

Hand, S., M. Archer, and H. Godthelp. 1997. First record of *Hydromops* (Microchiroptera: Molossidae) from Australia: its biocorrelative significance. *Mémoires et Travaux de l'Institut de Montpellier de l'Ecole Pratique des Hautes Etudes* 21: 153–162.

Hand, S., L. Dawson, and M. Augee. 1988. *Macroderma koppa*, a new Tertiary species of false vampire bat (Microchiroptera: Megadermatidae) from Wellington Caves, New South Wales. *Records of the Australian Museum* 40(6): 343–351.
https://doi.org/10.3853/j.0067-1975.40.1988.160

Hand, S. J., P. Murray, D. Megirian, M. Archer, and H. Godthelp. 1998. Mystacinid bats (Microchiroptera) from the Australian Tertiary. *Journal of Paleontology* 72: 538–545.
https://doi.org/10.1017/S0022336000024318

Hand, S. J., and B. Sigé. 2018. A new archaic bat (Chiroptera: Archaeonycteridae) from an Early Eocene forest in the Paris Basin. *Historical Biology* 30: 227–236.
https://doi.org/10.1080/08912963.2017.1297435

Kaňuch, P., T. Aghová, Y. Meheretu, R. Šumbera, and J. Bryja. 2015. New discoveries on the ecology and echolocation of the heart-nosed bat *Cardioderma cor* with a contribution to the phylogeny of Megadermatidae. *African Zoology* 50: 53–57.
https://doi.org/10.1080/15627020.2015.1021711

King, T. 2013. *First Australian Pliocene Sheathtail Bats (Chiroptera: Emballonuridae) with a Review of Emballonurid Palaeoecology and Distribution*. Unpublished B.Sc. (Hons) thesis. University of New South Wales, Sydney.

Mahoney J. A., M. J. Smith, and G. C. Medlin. 2008. A new species of hopping-mouse, *Notomys robustus* sp. nov. (Rodentia: Muridae), from cave deposits in the Flinders and Davenport Ranges, South Australia. *Australian Mammalogy* 29: 117–135.
https://doi.org/10.1071/AM07017

Menu, H., S. Hand, and B. Sigé. 2002. Oldest Australian vespertilionid (Microchiroptera) from the early Miocene of Riversleigh, Queensland. *Alcheringa* 26: 319–331.
https://doi.org/10.1080/03115510208619260

Molnar, R. E., L. S. Hall, and J. A. Mahoney. 1984. New fossil localities for *Macroderma* Miller, 1906 (Chiroptera: Megadermatidae) in New South Wales and its past and present distribution in Australia. *Australian Mammalogy* 7: 63–73.

Rasband, W. S. 1997–2005. *ImageJ*, U.S. National Institutes of Health, Bethesda, Maryland, USA. [Accessed 15 January 2020]
http://rsb.info.nih.gov/ij/

Ravel, A., M. Adaci, M. Bensalah, A.-L. Charruault, E. M. Essid, H. K. Ammar, W. Marzougui, M. Mahboubi, F. Mebrouk, G. Merzeraud, M. Vianey-Liaud, R. Tabuce, and L. Marivaux. 2016. Origine et radiation initiale des chauves-souris modernes: Nouvelles découvertes dans l'Éocène d'Afrique du Nord. *Geodiversitas* 38: 355–434.
https://doi.org/10.5252/g2016n3a3

Rowe, K. C., A. S. Achmadi, P.-H. Fabre, J. J. Schenk, S. J. Steppan, and J. A. Esselstyn. 2019. Oceanic islands of Wallacea as a source for dispersal and diversification of murine rodents. *Journal of Biogeography* 46: 2752–2768.
https://doi.org/10.1111/jbi.13720

Sevilla, P. 1990. Rhinolophoidea (Chiroptera, Mammalia) from the upper Oligocene of Carrascosa del Campo (Central Spain). *Geobios* 23: 173–188.
https://doi.org/10.1016/S0016-6995(06)80050-1

Sigé, B. 1968. Les Chiropteres du Miocene inférieur de Bouzigues. 1. Etude systématique. *Palaeovertebrata* 1: 65–133.
https://doi.org/10.18563/pv.1.3.65-133

Sigé B. 1976. Les Megadermatidae (Chiroptera, Mammalia) miocènes de Béni Mellal, Maroc. In: *Géologie Méditerranéenne* 3: 71–85.
https://doi.org/10.3406/geolm.1976.963

Sigé B. 2011. *Cryptobune* nov. gen., chiroptère carnivore des phosphorites du Quercy, SW France. *Bulletin de la Société d'histoire naturelle de Toulouse* 147: 47–54.

Sigé, B., S. Hand, and M. Archer. 1982. An Australian Miocene *Brachipposideros* (Mammalia, Chiropetra) related to Miocene representatives from France. *Palaeovertebrata* 12: 149–172.

Simmons, N. B., and A. L. Cirranello. 2020. *Bat Species of the World: A Taxonomic and Geographic Database*. [Accessed on 15 January 2020].
https://batnames.org/home.html

Smissen, P. J., and K. C. Rowe. 2018. Repeated biome transitions in the evolution of Australian rodents. *Molecular Phylogenetics and Evolution* 128: 182–191.
https://doi.org/10.1016/j.ympev.2018.07.015

Stephens, N. P., and D. Y. Sumner. 2003. Late Devonian carbon isotope stratigraphy and sea level fluctuations, Canning Basin, Western Australia. *Palaeogeography, Palaeoclimatology, Palaeoecology* 191: 203–219.
https://doi.org/10.1016/S0031-0182(02)00714-9

Teeling, E. C., M. S. Springer, O. Madsen, P. Bates, S. J. O'Brien, and W. J. Murphy. 2005. A molecular phylogeny for bats illuminates biogeography and the fossil record. *Science* 307: 580–584.
https://doi.org/10.1126/science.1105113

Woinarski, J. C. Z., A. A. Burbidge, and P. L. Harrison. 2014. *The Action Plan for Australian Mammals 2012*. Collingwood: CSIRO Publishing.
https://doi.org/10.1071/9780643108745

Woodhead, J., S. J. Hand, M. Archer, I. Graham, K. Sniderman, D. A. Arena, K. H. Black, H. Godthelp, P. Creaser, and E. Price. 2016. Developing a radiometrically-dated chronologic sequence for Neogene biotic change in Australia, from the Riversleigh World Heritage Area of Queensland. *Gondwana Research* 29: 153–167.
https://doi.org/10.1016/j.gr.2014.10.004

Worthington Wilmer, J., L. Hall, E. Barratt, and C. Moritz. 1999. Genetic structure and male-mediated gene flow in the Ghost Bat (*Macroderma gigas*). *Evolution* 53: 1582–1591.
https://doi.org/10.1111/j.1558-5646.1999.tb05421.x

Ziegler, R. 1993. Die Chiroptera (Mammalia) aus dem Untermiozän von Wintershof-West bei Eichstätt (Bayern). *Mitteilungen der Bayerischen Staatssammlung für Paläontologie und historische Geologie* 33: 119–154.